Available online at www.sciencedirect.com
SCIENCE DIRECT®

Journal of the European Ceramic Society 23 (2003) 1283–1291
www.elsevier.com/locate/jeurceramsoc

Preparation and crystallization of forsterite fibrous gels

M.T. Tsai*

Department of Materials Science and Engineering, National Huwei Institute of Technology, PO Box 385 Touliu, Yunlin 640, Taiwan

Received 3 April 2002; received in revised form 5 August 2002; accepted 19 August 2002

Abstract

Transparent forsterite fibrous gels were prepared from the hydrolysis of alkoxide precursor sols with acetic acid and water, and the crystallization process of gel fibers was studied after heat treatments up to 1500 °C. Appropriate amount of acetic acid not only promoted the formation of spinnable linear-type polymeric species, but also enhanced the chemical homogeneity and reduced the crystallization temperature of the resultant gels. On heating, fibrous gels started to crystallize into forsterite at 550 °C as investigated by infrared spectrum, X-ray diffraction and thermal analysis. Single phase forsterite fiber thus could be obtained up to 1500 °C when the amount of hydrolysis water was limited. However, fibrous gel derived from the high-water-content sol displayed a few secondary phases of the magnesia (MgO) and protoenstatite ($MgSiO_3$) following heating at 1000 and 1400 °C, respectively; similarly, xerogels derived from without or with insufficient amount of acetic acid also revealed the segregation of second phases on heating. The synthesized forsterite fibers displayed nanocrystalline structure up to 1100 °C. On heating to 1300 °C, fired fibers exhibited grain growth into around 0.3–0.5 μm in size, with the room temperature dielectric constants of around 6.8–7.2 (at 1 MHz).

Keywords: Fibres; Forsterite; Forsterite fibres; Microstructure-final; Sol-gel processes

1. Introduction

The production of ceramics via solid-state reactions usually requires high temperature and long reaction time. In the sol-gel processing, a solution of molecular precursors is converted by a hydrolysis–condensation reaction into a gel that on drying and densification gives the glass or ceramics material.[1] The sol-gel process is widely recognized that can provide molecular-level mixing for a high degree of homogeneity, which leads to lowering the crystallization temperature and preventing phase segregation during heating.[2,3] Also, the sol-gel route is one of the promising methods for producing nanocrystalline materials. However, in multicomponent silicate systems, the hydrolysis and condensation rates are different between silicon and the other alkoxides. This may cause nonuniform precipitation and chemical inhomogeneity of the gels, leading to higher crystallization temperature and undesired crystalline phases.[4] Chemical modification of metal alkoxides with organic agents has been used to overcome this limitation, since the processing properties of the start materials can be improved drastically. It has already been shown that metal alkoxides react with chelating agents, such as acetylacetone or ethylacetoacetate, giving rise to new molecular precursors that result in better control of the hydrolysis - condensation reaction.[4,5] Forsterite (Mg_2SiO_4) xerogel powders have been synthesized via the sol-gel method.[6–11] The chemical modification of forsterite precursor solution has been investigated by Mitchell et al.[10,11]

The chain-like or linear polymers are well known to be required for drawing the fibrous gels, while the formation of three-dimensional network structures would be favorable for the bulk or monolithic gels.[12] We have demonstrated that acetic acid is efficient for modifing the hydrolysis–condensation rate of the forsterite precursor alkoxide and for stabilizing the sol, leading to the generation of bidentate acetate ligands.[13] As a result, formation of gel fiber was achieved when sufficient amount of acetic acid was added either before or after hydrolysis of the alkoxide solution. The effects of hydrolysis processing on the characterization of forsterite gel

* Tel.: +886-5-5320731; fax: +886-5-6328863.
E-mail address: mttsai@ms23.hinet.net (M.T. Tsai).

0955-2219/03/$ - see front matter © 2002 Elsevier Science Ltd. All rights reserved.
PII: S0955-2219(02)00305-9

fibers have been studied.[13,14] However, previous studies [7–10] have shown that it is difficult to achieve homogeneous forsterite since the second phases such as magnesia (MgO) and enstatite ($MgSiO_3$) frequently formed during heating the gel powders at around 1200–1300 °C. The present work aims to further investigate the impact of acetic acid on the crystallization and on the homogeneity of fibrous gels following heating up to 1500 °C. It reveals that the use of an appropriate amount of acetic acid in the synthesis not only facilitates the drawing of fibers, but is also efficient for the production of single phase forsterite. The microstructural evolution of fired fibers is also explored.

2. Experimental procedure

The precursor solution with the oxide stoichiometry of forsterite was synthesized by dissolving a 21.5 wt.% methanol solution of magnesium methoxide in a 60 wt.% ethanol solution of tetraethylorthosilicate (TEOS). The mixed alkoxide solution was stirred and refluxed at 0–5 °C for 1 h, and then a mixture of deionized water and glacial acetic acid was added dropwise for hydrolysis; the concentrations of water and acetic acid were ranged in 0.5–5.0 and 0–1.0 molar ratio to TEOS, respectively. Following thorough stirring and refluxing for 4 h, the alkoxide solutions were kept open to further hydrolysis–condensation reaction at the ambient temperature. The solutions increased in viscosity with increase in standing time until gelation. Gelation time was measured as the time at which the maximum viscosity of the sol was reached under a constant shear rate. Transparent fibrous gels were obtained by immersing a glass rod into the viscous sols, then pulling it up by hand.

The shear-rate dependence of viscosities of the solutions was measured at 25 °C using a Brookfield viscometer equipped with a thermostat and an UL adaptor. The crystallization process of fibrous gel was studied by differential thermal analysis/thermogravimetry (DTA/TG; Seiko SSC 5000), powder X-ray diffractometry (XRD; Rigaku D/MAX-ÉÉÉ), and Fourier transform-infrared spectrometry (FT-IR; Bomen Michelson MB100); gel samples were air dried at 80 °C, then heated at 200–1500 °C for 2 h at a rate of 10 °C min^{-1}, and finally ground into fine powders before measurements were taken. Meantime, thermal analysis was performed in flowing air at a heating rate of 10 °C min^{-1}, infrared spectra with a resolution of 2 cm^{-1} were recorded in the 450–2000 cm^{-1} frequency range using the KBr method, and X-ray diffraction was measured with Ni-filtered CuKα radiation. The microstructures of the fired fibers were observed by scanning electron microscopy (SEM; Philip XL-40FEG), in which the fibrous gels were dried at room temperature and then heated at 800–1300 °C in air using a rate of 3 °C min^{-1}. The dielectric constant of the fired fiber was measured by a precision inductance–capacitance–resistance (LCR) meter (HP 4284A) at 1 MHz with silver electrodes attached to both ends of the fiber; for comparison, disk samples were uniaxially pressed from the relative gel-derived powders to obtain dielectric properties.

3. Results and discussion

3.1. Spinnability of sols

Table 1 lists the properties of solution samples with different concentrations of water and acetic acid. The gelation time decreased when the water content increased while the reverse effect was observed with acetic acid. The gelation rate was slowed down with increasing the concentration of acetic acid; thereby the stability of the sols is improved. For the water content ranging in 0.5–2.0 molar ratio to TEOS, solutions with an acetic acid/TEOS molar ratio above 0.5 showed spinnability, as in the cases of sols F1, F2 and F3. Spinnability did not occur when an insufficient amount of acetic acid was involved in the sols, regardless of water content. Furthermore, the transparency of the gels increased with the amount of acetic acid, as compared sample G1 with those of samples G3–G6. With lower water content and a small amount of acetic acid, sol G7 showed no spinnability and resulted in a translucent xerogel. Increasing the acetic acid concentration could improve the homogeneity and give a transparent aspect, as in the case of sample G8. However, if a large amount of water was added to the solution, as in the

Table 1
The influences of the amounts of acetate acid and water on the gelation time (t_{gel}), spinnability and appearance of gels

Samples	$[H_2O]$[a]	$[CH_3COOH]$[a]	t_{gel} (h)	Spinnability	Aspects[b]
G1	2.0	0	7.1	No	Xerogel, translucent
G2	2.0	0.05	8.0	No	Xerogel, translucent
G3	2.0	0.1	10.3	No	Xerogel, transparent
G4	2.0	0.2	14.6	No	Xerogel, transparent
G5	2.0	0.4	21.2	No	Xerogel, transparent
G6	2.0	0.5	24.7	Poor	Xerogel, transparent
F1	2.0	1.0	32.0	Yes	Fiber, transparent, ~10 cm
G7	0.5	0.1	14.5	No	Xerogel, translucent
G8	0.5	0.2	21.8	No	Xerogel, transparent
F2	0.5	0.5	45.3	Yes	Fiber, transparent, ~8 cm
F3	0.5	1.0	52.0	Yes	Fiber, transparent, ~30 cm
G9	5.0	0.2	⩽0.05	No	Xerogel, opaque

[a] Molar ratio to TEOS.
[b] After drying at room temperature.

case of G9, the sol became turbid and occurred gelation very fast. Higher water content significantly promoted the hydrolysis–condensation reaction and viscosity and thus enhanced the formation of a branched or three-dimensional network rather than a linear structure.[13] When acetic acid concentration was small and excess water was available, the hydrolysis rate became so high that gelation occurred locally. This would result in a turbid aspect of the gels.

The spinnable sols prepared with higher water content and/or lower amount of acetic acid also reflected the shortening of the drawn fibers as showed in Table 1. Higher amounts of acetic acid seemed to inhibit the formation of three-dimensional network polymers and to favor the formation of linear polymeric structures during gelation, since the spinnability improved significantly. It was observed that for sols with acetic acid concentration ranging from 0.5 to 1.0 molar ratio to TEOS, transparent fibrous gels could be obtained for molar ratios of water/TEOS = 0.5–2.0. This result was also similar to the previous study.[13] The use of acetic acid in the preparation not only enhances the spinnability but also increases the solubility of the precursor solution and resulted in a transparent sol during gelation.

Fig. 1 shows the change of viscosity with shear rate, based on various aging time, for the spinnable sol F1. The viscosity of the sol was independent of the shear rate (i.e. Newtonian flow behavior) to a high viscosity range and then slightly decreased with the shear rate (i.e. slightly shear-thinning behavior) after 31 h of aging. With further aging to $t = 31.8$ h, a thixotropic flow characteristic could be observed and followed the occurrence of gelation quickly. The results shown in Fig. 1 were the typical flow behaviors of the investigated spinnable sols, but they remained Newtonian or near Newtonian flow behaviors to higher viscosities when lower water content was used, as in the case of sample F3 (Table 1). The viscosity suitable for spinning was observed between around 10 and 100 poise for the spinnable sols investigated in the present study. The cross-sections of those dried fibrous gels were circular, ellipsoidal or dumbbell in shape with diameters ranged of 20–200 μm. The diameter of the fibers was mainly dependent on the drawing rate, while the length of the fibers was affected by the solution concentration, as shown in Table 1. Rheological measurements suggested that the sols exhibited spinning when they were viscous and Newtonian or near Newtonian until near the time of gelation. The sols became unspinnable when thixotropic flow behaviors were observed. In the viscosity range suitable for spinning, those unspinnable sols exhibit strongly shear-thinning and thixotropic flow behaviors.[13]

3.2. IR spectra of gels

Fig. 2 shows the infrared spectra of the processed xerogel and fibrous gel samples after dried at 80 °C. Notably, the bands around 1500 cm^{-1}, in which fibrous gels F3 and F1 as shown in Fig. 2a and b was found to have well defined doublet peaks at 1595, 1536, 1442 cm^{-1} and 1576, 1438 cm^{-1}, respectively. According to the literature[15,16] and the previous study,[11] which could be due to bidentate acetate ligands. For fibrous gel F3, the frequency separation with $\Delta\nu = 153$ cm^{-1}, between

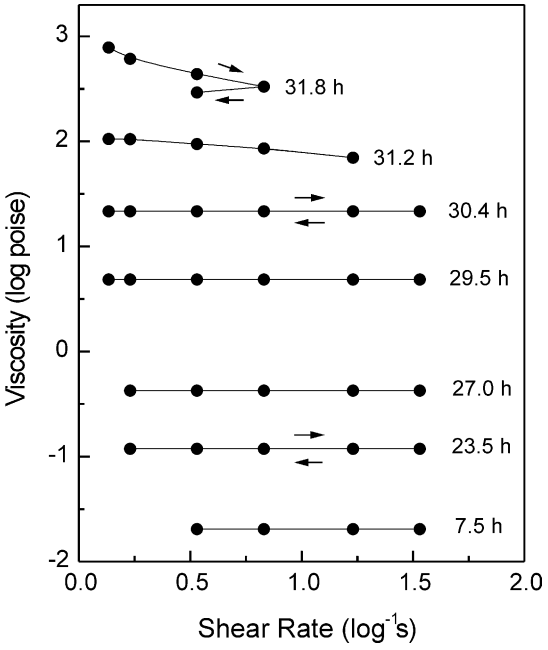

Fig. 1. Dependence of viscosity on shear rate for sol F1 obtained from various reaction times at 25 °C.

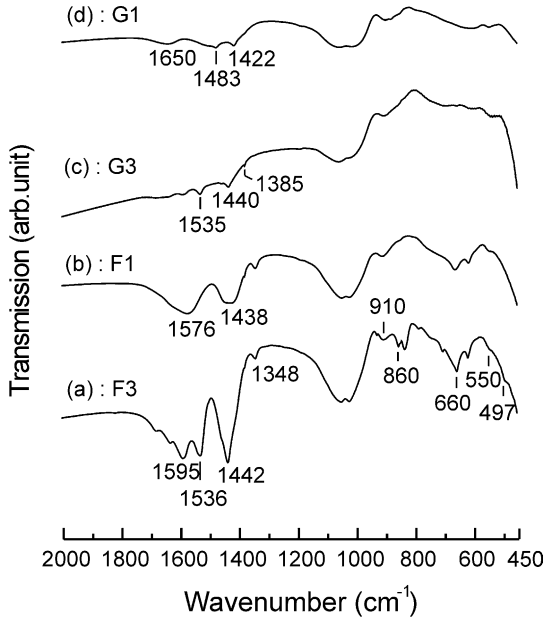

Fig. 2. Infrared spectra of dried (a) fibrous gel F3, (b) fibrous gel F1, (c) xerogel G3, and (d) xerogel G1.

the stretching asymmetric ν_{asym} (COO) vibration at 1595 cm^{-1} and the stretching symmetric ν_{sym} (COO) vibration at 1442 cm^{-1} as shown in Fig. 2a, suggests that acetate anions act as bridging bidentate ligands because the frequency separation of bridging acetate usually lay between 120 and 160 cm^{-1};[13,14] and a smaller doublet with $\Delta\nu = 94$ cm^{-1}, between the ν_{asym} (COO) at 1536 cm^{-1} and the ν_{sym} (COO) at 1442 cm^{-1}, corresponds to chelating bidentate ligands because the frequency separation of chelating acetate was usually smaller than that of bridging acetate.[15] Similarly, fibrous gel F1 (Fig. 2b) shows the frequency separation of $\Delta\nu = 138$ cm^{-1} between the ν_{asym} (COO) at 1576 cm^{-1} and the ν_{sym} (COO) at 1438 cm^{-1} that was also consistent with bidentate acetate ligands, but its larger value suggests bridging acetates rather than chelating acetates.[15,16] Fibrous gel derived from the high-water-content sol, i.e. sample F1 (Fig. 2b), revealed the reduction in both intensity and type of the doublets as compared with those of sample F3 (Fig. 2a). This could be considered mainly due to the breaking of the acetate ligands because a higher water content was contained during hydrolysis. It has been showed that a sufficient degree or concentration of acetate ligands was required to enhance the formation of linear-type molecular structures rather than three-dimensional networks in the viscous sols.[11] Furthermore, in addition to spinnability, fiber length also was considered to relate with the concentration of acetate ligands.[13] Accordingly, comparing the spectra in Fig. 2a and b, it was suggested that fibrous gel F1 had a lower degree of linear-type structures than that of F3 in light of a lower concentration of acetate ligands. This is reflected on fibrous gel F1 with shorter length than that of F3 as showed in Table 1. For both the fibrous gels, peaks at around 1690–1688 cm^{-1} and 1348 cm^{-1} corresponded to free acetic acid or probably due to the unidentate acetate.[16] This indicate that the acetic acid could also act as a dissolving agent when it was added during hydrolysis of the precursor solution.[17]

Xerogel G3 as shown in Fig. 2c, displaying characteristic absorption bands due to the ν_{asym} (COO) at 1597 and 1535 cm^{-1}, and to the ν_{sym} (COO) at 1440 cm^{-1}, respectively. This result suggested that bridging acetate ($\Delta\nu = 157$ cm^{-1}) and chelating acetate ($\Delta\nu = 95$ cm^{-1}) might occur.[15] However, its precursor solution became an elastic gel without showing any spinnability during gelation. The much lower degree or extent of acetate ligands might be one possible explanation for this difference in spinnability because of weak intensity in their characteristic peaks. Fig. 2d gives the infrared spectrum recorded on xerogel G1, which was prepared from the solution without acetic acid, showing remaining OR groups (absorptions at around 1483,1422 and 1385 cm^{-1} [18,19]) and the adsorption due to water around 1650 cm^{-1}.[18,20] No peaks related to acetate ligands were observed in this case. Comparing the spectra in Fig. 2b–d, it also observed that the residual OR groups reduced in intensity with increasing amounts of acetic acid, indicating OR groups were replaced by acetate ligands. It is considered that the replacement of alkoxy groups by acetate anions occurred during the hydrolysis–condensation process, which would lead to the formation of soluble molecular species and bidentate acetate ligands.[13] The bidentate acetate ligand groups are then slowing down both hydrolysis and condensation reactions, decreasing therefore the gelation rate.

In addition, characteristic bands shown in Fig. 2 related to the $Si–O^-$ anionic network structures were observed around 1055–490cm^{-1}; in which bands around 1055–1020 cm^{-1} were attributed to asymmetric Si–O–Si stretching modes;[18,20] bands around 910 cm^{-1} were assigned to the stretching vibrations of nonbridging Si–OH;[18] the band at 860 cm^{-1} was also assigned to stretching vibrations of Si–OH bonds;[22] bands in the range of 840–650 cm^{-1} corresponded to Si–O–Si symmetric stretching vibrations,[18,20] in which the band at 790 cm^{-1} was also associated to vibration modes of ring structure of SiO_4 tetrahedra;[18,23] the band around 550 cm^{-1} was assigned to the modes of MgO_4 in the Si–O–Mg linkages;[13,21,24] the band around 497 cm^{-1} was assigned to a Si–O–Si bending mode.[21,23] Peaks around 660 and 625 cm^{-1} were associated with the deformation vibrations of OCO and the out-off-plane bending vibration modes of CH or COO,[25] respectively.

3.3. Fibrous gel to ceramic fiber transition

Fig. 3 shows the infrared spectra of fibrous gel F3 heated at various temperatures for 2 h. The infrared

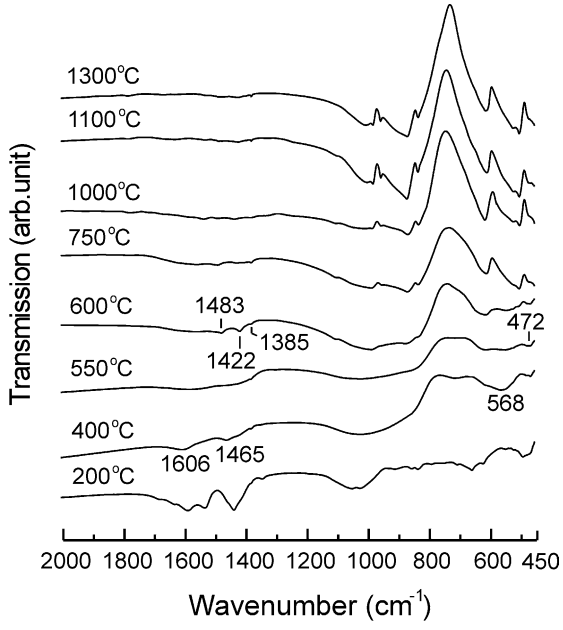

Fig. 3. Infrared spectra of fibrous gel F3 heated for 2 h at various temperatures in air.

spectra on heating the fibrous gel indicate that a further condensation may occur between silanol groups and decomposition of acetate ligand groups. Continued condensation with temperature is indicated from the reduction in the relative intensity of the band around 910 and 860 cm^{-1} assigned to Si–OH stretching[18,22] along with a progressive decrease in the intensity of the characteristic peaks of acetate ligands around 1500 cm^{-1}. The characteristic peaks of acetate ligands decreased in intensity with heating and gradually disappeared above 400 °C. On heating at 400 °C, a residual frequency separation of $\Delta\nu = 141$ cm^{-1} corresponded to bridging acetates, between the ν_{asym} (COO) at 1606 cm^{-1} and the ν_{sym} (COO) at 1465 cm^{-1}, was observed. It seems to suggest that bridging acetates were more difficult to remove than that of chelating acetates on heating. On the other hand, the weak shoulder around 550 cm^{-1}, presumably assigned to the modes of MgO_4 in the Si–O–Mg linkages,[13,21,24] showing an increase in the intensity up to 400 °C. Simultaneously, the band due to SiO_4 bending around 497 cm^{-1} also increased in intensity at 200 °C and substantially decreased at 400 °C; instead, appearing a broad band with stronger absorption around 568 cm^{-1} and a new peak around 470 cm^{-1} corresponding to MgO_6 modes.[26] With further heating at 550 °C, the band around 568 cm^{-1}decreased in intensity but the band around 470 cm^{-1} retained in the same position, and some of the characteristic peaks of crystalline forsterite started to show at around 472, and 616 cm^{-1}.[26,27] With further heating at 600 °C, those peaks due to crystalline forsterite became more obvious, meanwhile, the bands corresponding to C-H vibration modes around 1385, 1422 and 1483 cm^{-1} [18,19] were visible, which was mainly due to the combustion of the organic groups. Above 750 °C, the bands related to the characteristic peaks of well-crystallized forsterite appear at 1007, 986, 960, 873, and 838 cm^{-1} (SiO_4 stretching), at 616, 527, and 507 cm^{-1} (SiO_4 bending), and at 475 cm^{-1} for modes of octahedral MgO_6. The band positions for forsterite agreed with the results of previous investigations.[26,27] On heating fibrous gels F1 and F2, a similar trend of the IR spectra was observed.

Figs. 4 and 5 show the X-ray diffraction patterns of xerogel G1 and fibrous gels F1 and F3 after firing at various temperatures. These samples were essentially amorphous after drying and xerogel G1 (Fig. 4a) remained in the amorphous state up to 600 °C, while the fibrous gels started to crystallize into the forsterite phase [28] at a temperature as low as 550 °C (Figs. 4b and 5). On heating the xerogel, Fig. 4a shows that the traces of magnesia (MgO) (200) peak[29] and protoenstatite ($MgSiO_3$) (121) and (310) peaks[30] are detected following heating at 750 and 1300 °C, respectively. A similar trend of the XRD results also was observed for the other xerogels (Table 1). For fibrous gel F1, similarly, Fig. 4b shows that the traces of MgO and $MgSiO_3$ can also be detected following heating at 1000 and 1400 °C, respectively. However, single phase forsterite fiber can be obtained up to 1500 °C for the fibrous gel derived from the low-water-content sol. As shown in Fig. 5, forsterite also began to crystallize at 550 °C for fibrous gel F3; the crystallinity of forsterite increased with heat-treatment temperatures and other crystalline phases were not detected up to 1500 °C. This result was consistent with the appearance of the characteristic peaks of crystallite forsterite in the IR spectra as shown in Fig. 3.

In the chemical solution route, molecular-level mixing is important in lowering the crystallization temperature and preventing phase segregation during heating. However, the hydrolysis rate of magnesium alkoxide is much faster than that of silicon alkoxide may cause chemical heterogeneity in the gel samples. Burlitch et al.[6] prepared forsterite gel powders by hydrolyzed a mixture of TEOS, magnesium, and methanol with hydrogen peroxide, and observed the homogeneous crystallization of forsterite up to 1000 °C; Kazakos et al.[7] found that the secondary phase (enstatite) could be detected only after heating to above 1200 °C; Ban et al.[8] observed also the beginning crystallization of forsterite at 500 °C and did not detect other crystalline phase up to 1300 °C, but prolonged heating led to the formation of enstatite; Mitchell et al.[9–11] showed that even by partial prehydrolysis of TEOS and operating in a chelating solvent, 2-methoxyethanol, magnesia and enstatite were observed in addition to forsterite when heated the gel powders at 1200 °C. In the present work, acetic acid apparently has a positive effect on the chemical homogeneity and on the reduction of the crystallization temperature.

The lower crystallization temperature as demonstrated from a comparison of Fig. 4b (i.e. fibrous gel F1) with 4a (i.e. xerogel G1) reflected that the used of acetic acid in the synthesis could promote the intimate mixing of the colloidal particles. For fibrous gels F1 and F3, the appearances of the two spinnable sols were homogeneous and clear, and the formation of glassliked transparent fibrous gels in all the cases investigated while it was translucent for xerogel G1. This suggested that both magnesium and silicon ions were more uniformly distributed in fibrous gels F1 and F3 than those in xerogel G1. The lower crystallization temperature shown in Figs. 4b and 5 is partly responsible for the above suggestion. Namely, the appropriate amount of acetic acid can lead to more intimate mixing of the precursor sols, gives rise to form clear sols, which in turn leads to the crystallization of forsterite at lower temperature. However, the secondary phases of MgO and $MgSiO_3$ were observed on heating xerogel G1 and fibrous gel F1, indicating a lesser degree of homogeneity than that of fibrous F3. For fibrous gel F1, acetic acid could improve the homogeneous state of the sols but high water content seemed to be segregating MgO clusters in forsterite during heating. The MgO could further

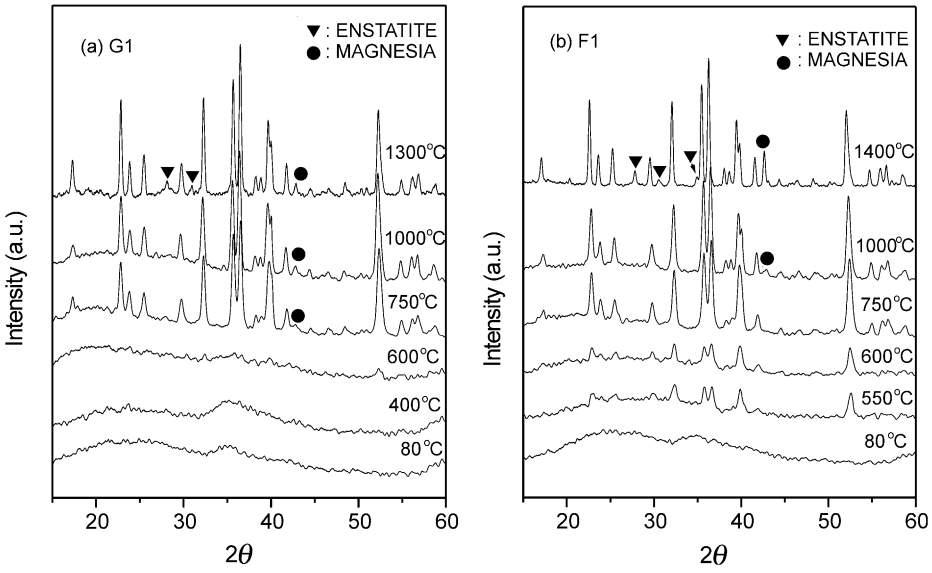

Fig. 4. X-ray diffraction patterns of (a) xerogel G1 and (b) fibrous gel F1 fired at various temperatures for 2 h.

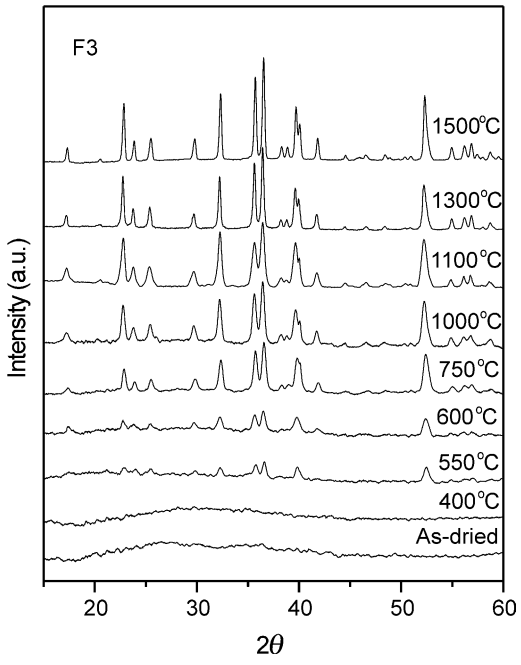

Fig. 5. X-ray diffraction patterns of fibrous gel F3 fired at various temperatures for 2 h.

react with the residual amorphous silica via the solid diffusion reaction to form $MgSiO_3$ as proposed by Brindley and Hayami.[31] However, X-ray diffraction results suggested that there essentially existed a different level of homogeneity and /or ultrastructures in both the fibrous gels following heating although the crystallinities were similar in both the cases investigated. For fibrous gels prepared with lower amount of acetic acid, as in the case of sample F2 (Table 1), the XRD results were the same as that of sample F1. This meant that appropriate amount of acetic acid was essential for producing homogenous fibrous gels. High water content and/or low acetic acid concentration could influence the reproducibility of homogeneous forsterite, meaning that the occurrence of local chemical inhomogeneity was possible when the fibrous gel prepared with such conditions. Certainly, however, if less water content and the appropriate amount of acetic acid were used, and homogeneous forsterite fibers with good reproducibility might result.

Fig. 6 shows TG and DTA curves for xerogel G1 and fibrous gels F1 and F3, respectively. Both fibrous gels F1 and F3 show four distinct steps of weight loss in the TG curves (Fig. 6a), The first around 30–180 °C was mainly due to the evaporation of water, free acetic acid or residual organics corresponding to a broad endothermic peak around 69–72 °C in the DTA curves (Fig. 6b). The second around 200–500 °C involved about 16.3–13.8 wt.% weight loss and a sharp exothermic peak around 470 °C for both the samples. This step may be due to the liberation of hydroxyl groups, alcohol and acetate groups, and their combustion. This is also consistent with the IR spectra, indicating that continued condensation with temperature can occur between silanol groups and decomposition of acetate ligand groups. The third step around 510–620 °C involved about 13.3–8.5 wt.% significant weight loss for both the samples and also accompanied a sharp exothermic peak around 538–546 °C in the DTA curves. According to the X-ray diffraction results (Figs. 4b and 5), crystallization began at 550 °C. Also, infrared spectra revealed that the combustion and decomposition of residual organic groups occur at 400–600 °C, as peaks appeared around 1385, 1422 and 1483 cm^{-1} (Fig. 3). From these results, the third step suggested that the combustion of residual organic groups and the further condensation reaction could induce the conversion of amorphous fibrous gels into crystalline forsterite.[14] The

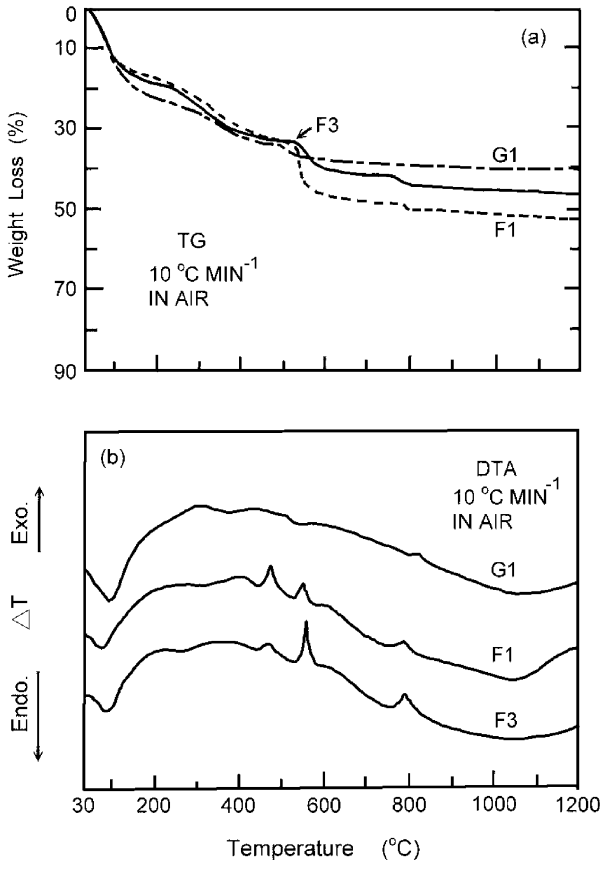

Fig. 6. (a) TG and (b) DTA curves for xerogel G1 and fibrous gels F1 and F3 predried at room temperature.

fourth step around 770–820 °C involved a small weight loss of about 2.3–1.4 wt.% and an exothermic peak around 781–779 °C in the DTA curves of both the samples. This step may be considered to be the decomposition or combustion of residual C–H groups proceeding during firing. The transparent fibrous gels turned black upon heating above 200 °C and then white after 1000 °C, supporting the above observation. Both the fibrous gels could be regarded as essentially similar in their thermal reactivity, which is consistent with the XRD results.

For xerogel G1, weight loss occurred in three main steps (Fig. 6a). The first around 30–180 °C involved about 22.6 wt.% weight loss and the second around 200–490 °C involved about 11.7 wt.% weight loss, and accompanied a broad endothermic peak around 88 and 360 °C in the DTA curve, respectively (Fig. 6b); The third step around 500–600 °C involved about 4.1 wt.% weight loss, and accompanied an endothermic peak around 520 °C in the DTA curve; these results probably due to the loss of water and residual organics. There was no further significant weight loss above 600 °C. A weak trace of exothermic peak around 810 °C probably related to the decomposition or combustion of residual organics.

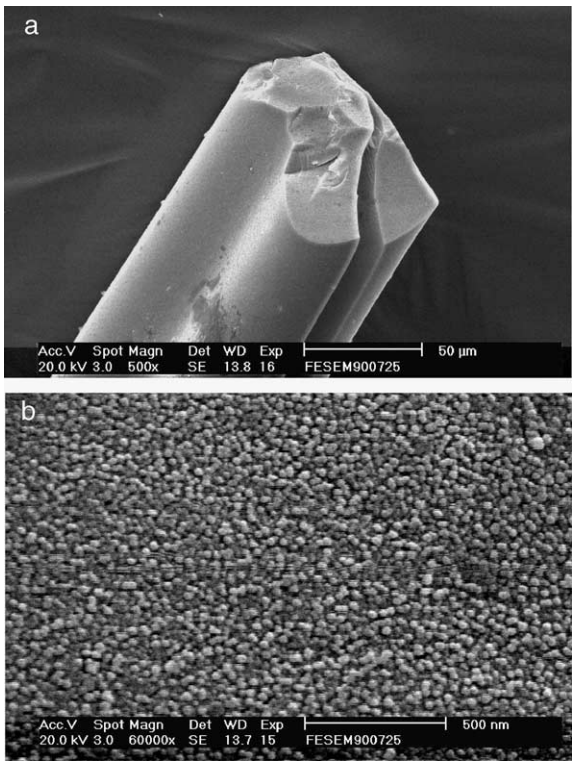

Fig. 7. Scanning electron micrographs of fibrous gel F3 after heating at (a) 800 °C, and (b) is a higher magnification of (a), showing the nanocrystalline microstructures.

3.4. Nanostructure of forsterite fiber

Fig. 7 shows the microstructures of heating fibrous gel F3 at 800 °C for 2 h. The fired fiber exhibited very dense structure both on the surface and a fracture surface, but the fiber surfaces frequently displayed a few cracks. The observed defects in the fired fibers were probably related to the combustion of the residual organics and to the removal of the volatile substances. Since the fibrous gels stiffened and became denser on heating, expelling the volatile substances from the solidified gels at higher temperature might produce some defects on both the surface and a cross section.[14] Under higher magnification, Fig. 7b shows that the fired fiber comprised nanocrystals of around 20–30 nm in size, revealing that the fired fiber is with a nanocrystalline structure upon heating at 800 °C. On heating to 1100 °C, the fired fiber still consists of nanocrystals of less than 100 nm in size as shown in Fig. 8a. However, the grain growth evidently occurred when heated the gel fibers at 1300 °C as shown in Fig. 8b. As shown, the fired fiber comprised crystals of around 0.3–0.5 μm in size; the average grain size was approximately 0.35 μm determined using the linear intercept method.[32] SEM observations revealed the fired forsterite fibers retaining nanocrystalline structures up to 1100 °C. On heating fibrous gels F1 and F2, a similar trend of the microstructural evolution was observed; the fired fibers also retained nanocrystalline structures up to

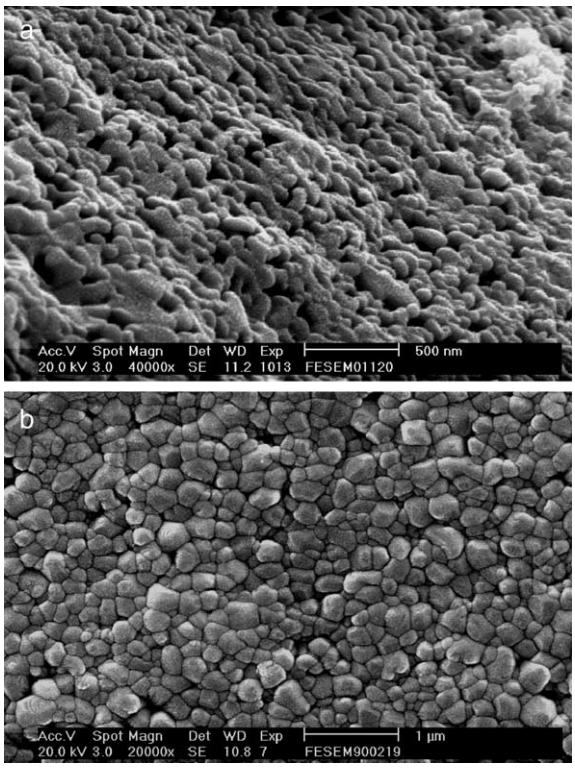

Fig. 8. Scanning electron micrographs of fibrous gel F3 after heating at (a) 1100 °C, and (b) 1300 °C, showing the fine-grained structures.

1100 °C with the same crystal size as that of fiber F3. After heating at 1300 °C, the average grain size of fiber F1 was somewhat larger than that of fibers F2 and F3.

Following heating at 1300 °C, the dielectric constant at room temperature of fibers F1 and F3 were in the range of about 7.2 (±0.6) and 6.8 (±0.7), at 1 MHz, respectively. The dielectric constant of fiber F2 was similar to that of fiber F1. These values were comparable to the respective disk sample values of about 5.6–7.0. These measured results reflected the low dielectric characteristics of the fired fibers. This suggests the potential applications of the materials in electronic packages[33] and /or fiber-reinforced composites. Further investigations of their mechanical and thermal properties are needed for possible use as reinforcements. However, the need for miniaturization of electronic and structural components will certainly continue, the sol-gel ceramic materials of forsterite in the fibrous forms thus may increase their applications in small-scale devices.

4. Conclusions

Acetic acid can significantly modify the hydrolysis-condensation reaction of the forsterite precursor alkoxide solutions, playing an important role in the formation of spinnable linear-type polymeric species. Bridging and chelating acetates are retained in the dried gels and can be removed upon heating above 400 °C.

In addition to spinnability, acetic acid can also used to improve the chemical homogeneity and to reduce the crystallization temperature of forsterite. However, high water content can promote the hydrolysis–condensation reaction and induces the occurrence of local chemical inhomogeneity, resulting in the formation of secondary phases such as magnesia and protoenstatite on heating. The appropriate amount of acetic acid and a low water content were essential for preparing fibrous gel, and homogeneous forsterite fibers with good reproducibility result.

Acknowledgements

The author would like to thank the National Science Council of the Republic of China for financially supporting this research in part under Contract No. NSC91-2216-E150-001.

References

1. Dislich, H., New routes to multicomponent oxide Glasses. *Angew. Chem. Int. Ed.*, 1971, **10**, 363–369.
2. Mehrotra, R. C., Chemistry of alkoxide precursors. *J. Non-Cryst. Solids*, 1990, **121**, 1–6.
3. Mackenzie, J. D., Application of the sol-gel process. *J. Non-Cryst. Solids*, 1988, **100**, 162–168.
4. Livage, J., Babonneau, F., Chatry, M. and Coury, L., Sol-gel synthesis and NMR characterization of ceramics. *Ceram. International*, 1997, **23**, 13–18.
5. Nass, R. and Schmidt, H., Synthesis of an alumina coating from chelated aluminum alkoxides. *J. Non-Cryst. Solids*, 1990, **121**, 329–333.
6. Burlitch, J. M., Beeman, M. L., Riley, B. and Kohlstedt, D. L., Low-temperature syntheses of olivine and forsterite facilitated by hydrogen peroxide. *Chem. Mater.*, 1991, **3**, 692–698.
7. Kazakos, A., Komarneni, S. and Roy, R., Preparation and densification of forsterite (Mg_2SiO_4) by nanocomposite sol-gel processing. *Mater. Lett.*, 1990, **9**, 405–409.
8. Ban, T., Ohya, Y. and Tokahashi, Y., Low-temperature crystallization of forsterite and orthoenstatite. *J. Am. Ceram. Soc.*, 1999, **82**, 22–26.
9. Mitchell, M. B. D., Jackson, D. and James, P. F., Preparation of forsterite (Mg_2SiO_4) powders via an aqueous route using magnesium salts and silicon tetrachloride ($SiCl_4$). *J. Sol-Gel Sci. Technol.*, 1999, **15**, 211–219.
10. Mitchell, M. B. D., James, P. F. and Jackson, D., Preparation and characterization of forsterite (Mg_2SiO_4) xerogels. *J. Sol-Gel Sci. Technol.*, 1998, **13**, 359–364.
11. Mitchell, M. B. D., Jackson, D. and James, P. F., Preparation and characterization of forsterite (Mg_2SiO_4) aerogels. *J. Non-Cryst. Solids*, 1998, **225**, 125–129.
12. Sakka, S. and Yoko, T., Fibers from gels. *J. Non-Cryst. Solids*, 1992, **147–148**, 394–403.
13. Tsai, M. T., Effects of hydrolysis processing on the characterization of forsterite gel fibers: É, preparation, spinnability and molecular structure. *J. Eur. Ceram. Soc.*, 2002, **22**, 1073–1083.
14. Tsai, M. T., Effects of hydrolysis processing on the characterization of forsterite gel fibers: II, crystallites and microstructural evolutions. *J. Eur. Ceram. Soc.*, 2002, **22**, 1085–1094.

15. Nakamoto, K., *Infrared and Raman Spectra of Inorganic and Coordination Compounds*, 4th ed. John Wiley and Sons, New York, 1986.
16. Alcok, N. W., Tracy, V. M. and Waddington, T. C., Acetates and aectato-complexes. ÉÉ. *Spectroscopic studies. J. Chem. Soc. Dalton, 1976, 2243–2249*.
17. Suzuki, H., Sato, H. and Hayashi, H., Properties of ZrO_2 gels prepared by controlled chemical modification method of alkoxide. *Mat. Res. Soc. Symp. Proc*, 1992, **271**, 83–88.
18. Orcel, G., Phalippou, J. and Hench, L. L., J. Structural changes of silica xerogels during low temperature dehydration. *J. Non-Cryst. Solids*, 1986, **88**, 114–130.
19. Sales, M. and Alarcon, J., Crystallization of sol-gel-derived glass ceramic powders in the CaO–MgO–Al_2O_3–SiO_2 System. *J. Mater. Sci*., 1994, **29**, 5153–5157.
20. Brinker, C. J. and Scherer, G. W., *Sol-Gel Science*. Academic Press, New York, 1990.
21. Mazza, D., Lucco-Borlora, M., Bussa, G. and Delmastro, A., High-quartz solid-solution phases from xerogels with composition $2MgO–2Al_2O_3–5SiO_2$ (μ-Cordierite) and $Li_2O–Al_2O_3–nSiO_2$ (n = 2 to 4) (β- Eucryptite): characterization by XRD, FTIR and surface measurements. *J. Eur. Ceram. Soc*., 1993, **11**, 299–308.
22. Nogami, M., Ogawa, S. and Nagasaka, K., Preparation of cordierite glass by the sol-gel process. *J. Mater. Sci*., 1989, **24**, 4339–4342.
23. Decottiganies, M., Phalippou, J. and Zarzycki, J., Synthesis of glasses by hot-pressing of gels. *J. Mater. Sci*., 1978, **13**, 2605–2618.
24. Gabelica-Robert, M. and Trate, P., Vibrations spectrum of akermanite-like silicates and germanates. *Spectrochimica Acta*, 1979, **35A**, 649–654.
25. Yoko, T., Kamiya, K. and Tanaka, K., Preparation of multiple oxide $BaTiO_3$ fibers by the sol-gel method. *J. Mater. Sci*., 1990, **25**, 3922–3929.
26. Lan, P. K., Yu, R., Lee, M. W. and Sharma, S. K., Structural distortions and vibration modes in Mg_2SiO_4. *Am. Mineral*., 1990, **75**, 109–119.
27. Jeanolz, R., Infrared spectra of olivine polymorphs: α, β phase and spinel. *Phys. Chem. Minerals*, 1980, **5**, 327–341.
28. *Powder Diffraction File*, Card No.34-189. JCPDS International Center for Diffraction Data, Swarthmore, PA, 1993.
29. *Powder Diffraction File*, Card No. 4-829. JCPDS International Center for Diffraction Data, Swarthmore, PA, 1992.
30. *Powder Diffraction File*, Card No. 11-273. JCPDS International Center for Diffraction Data, Swarthmore, PA, 1992.
31. Brindley, G. W. and Hayami, R., Kinetics and mechanism of formation of forsterite (Mg_2SiO_4) by solid state reaction of MgO and SiO_2. *Phil. Mag*, 1965, **12**, 505–514.
32. Mendelson, M. I., Average grain size in polycrystalline ceramics. *J. Am. Ceram. Soc*., 1969, **52**, 443–446.
33. Mukherjee, S. P., Suryanarayana, D. and Strope, D. H., Sol-gel processing in electronic packaging materials. *J. Non-Cryst. Solids*, 1992, **147–148**, 783–791.